

AD-A238 016

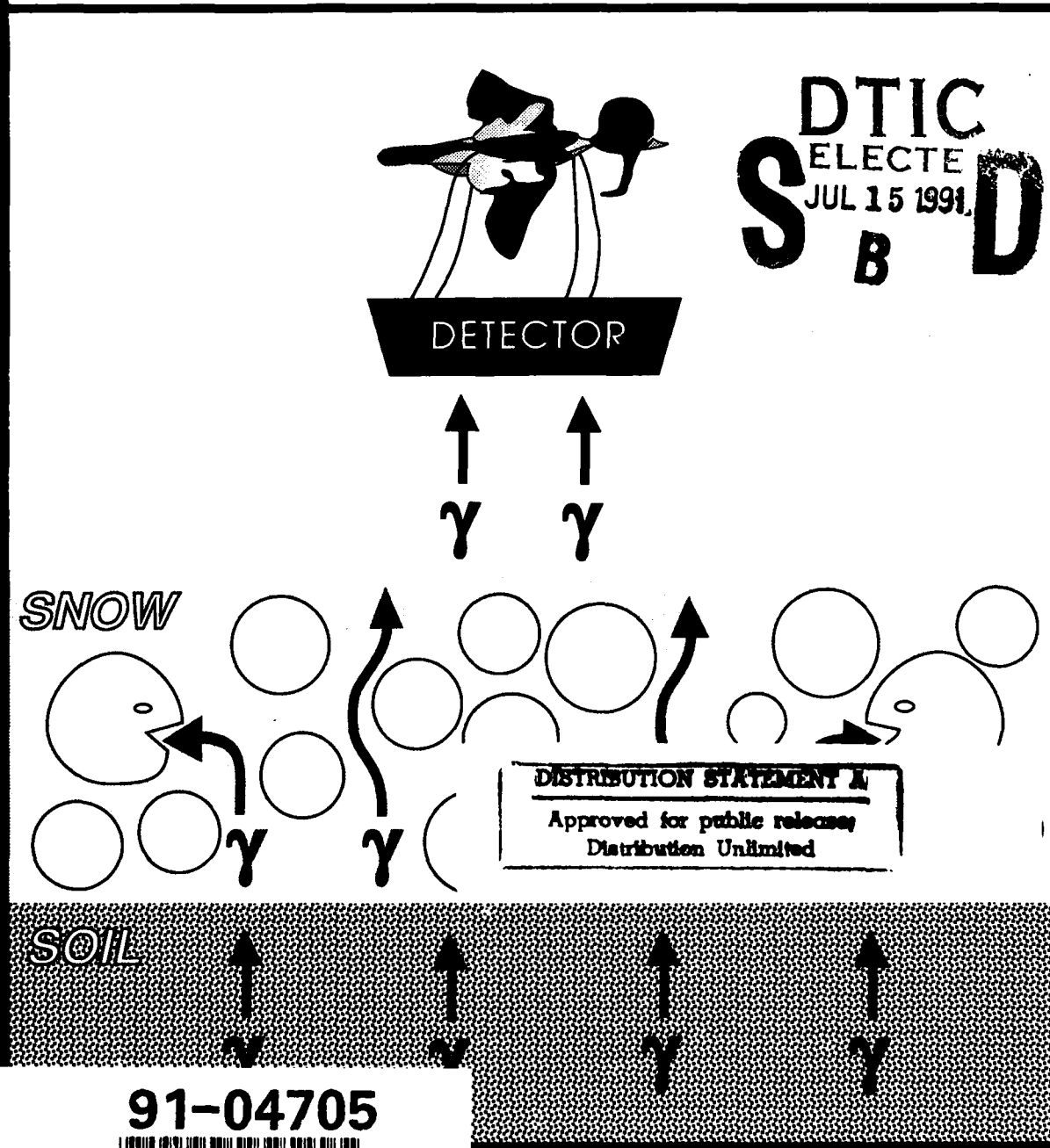


2

Remote Sensing of Snow Covers Using the Gamma-Ray Technique

Elmer L. Offenbacher and Samuel C. Colbeck

April 1991



91-04705



*For conversion of SI metric units to U.S./British customary units
of measurement consult ASTM Standard E380, Metric Practice
Guide, published by the American Society for Testing and
Materials, 1916 Race St., Philadelphia, Pa. 19103.*



**U.S. Army Corps
of Engineers**
Cold Regions Research &
Engineering Laboratory

Remote Sensing of Snow Covers using the Gamma-Ray Technique

Ter L. Offenbacher and Samuel C. Colbeck

April 1991

Shared for
OFFICE OF THE CHIEF OF ENGINEERS

Approved for public release; distribution is unlimited.

PREFACE

This report was prepared by Dr. Elmer L. Offenbacher of the Physics Department of Temple University and Dr. Samuel C. Colbeck of CRREL. Dr. Offenbacher prepared the original version of this report while at CRREL on the Summer Faculty Assessment program in 1983. Dr. Colbeck's participation in the preparation of this report was sponsored at CRREL by the Office of the Chief of Engineers under DA Project 4A762784AT42, *Cold Regions Engineering Technology*, Work Unit FS/003, *Radiational Effects on Snow Signatures*. Dr. Offenbacher's participation was funded under DA Project 4A762730AT42, *Design, Construction and Operations Technology for Cold Regions*, Work Unit D/004, *Seasonal Change in Strength and Stiffness of Soils and Base Courses*. This report was technically reviewed by Dr. T.R. Carroll and Dr. R.L. Grasty.

The contents of this report are not to be used for advertising or promotional purposes. Citation of brand names does not constitute an official endorsement or approval of the use of such commercial products.



Accession For	
NTIS GRA&I	<input checked="" type="checkbox"/>
DTIC TAB	<input type="checkbox"/>
Unannounced	<input type="checkbox"/>
Justification	
By _____	
Distribution/	
Availability Codes	
Dist	Avail and/or Special
A-1	

CONTENTS

	Page
Preface	ii
Introduction	1
Snow-water equivalent	2
Interaction of gamma rays with water substance	3
Sources of terrestrial gamma radiation	5
Variation of gamma activity with time	5
The airborne spectrum	6
Attenuation measurements near the ground	7
Technical aspects of airborne gamma-ray surveys	8
Equation for the transport of uncollided gamma rays	8
Reduction coefficients and the "working" equation	9
Techniques for determining SWE	10
Two-flight surveys	11
Spectral shape methods: single flights	13
Accuracy of D	14
Possible sources of error for any snow course	14
Additional sources of errors for the two-flight method	15
Additional time-dependent errors	15
Operational use	15
Conclusions	16
Annotated bibliography	16
Abstract	19

ILLUSTRATIONS

Figure

1. Gamma attenuation with depth of snow cover at three snow densities	2
2. Variation of snow-water equivalent across an open field	3
3. Mass absorption coefficient of water as a function of gamma-ray energy	4
4. Gamma cross sections for water, soil and air	4
5. Relative cosmic and terrestrial components of measured gamma flux as a function of altitude at Steamboat Springs, Colorado	5
6. Apparent uranium activity on the ground during a snowstorm	6
7. Airborne spectrum of energy peaks produced by radioactive elements in the ground	7
8. Snow-water equivalent vs one-hour gross gamma counts, measured 2 m above the ground	7
9. Geometric relationship for aerial gamma measurement	8
10. Potassium peak variation with aircraft altitude	10
11. Snow-water equivalent vs net count rate at altitudes from 61 to 300 m	12
12. Terrestrial gamma radiation spectra	13

TABLES

Table	Page
1. Typical terrestrial gamma radiation field	5
2. Mass attenuation coefficients and half thicknesses for air, water and rock at the photopeak energies of K^{40} , Bi^{214} and Tl^{208}	10
3. Values for α_w	10
4. Techniques of SWE measurements	11
5. Relative standard errors of snow surveying with various degrees of snow cover nonuniformity and various average snow-water equivalents along the flight line	15

Remote Sensing of Snow Covers Using the Gamma-Ray Technique

ELMER L. OFFENBACHER AND SAMUEL C. COLBECK

INTRODUCTION

The seasonal snow cover significantly influences agriculture, climate and the supply of water in many parts of the world. Accurate measurements of temporal and spatial snow cover variations are crucial for managing river flow and lake levels, using hydroelectric power facilities efficiently and forecasting floods. The importance of measuring the total water content of snow, or snow-water equivalence (SWE), was emphasized by NASA's Snowpack Properties Working Group (NASA 1982). This report classifies nine snow cover properties according to their usefulness in 18 diverse fields of application of snow cover information. SWE is the most sought-after value among these nine properties.

SWE and the snow-covered area are needed by hydrologists on a near-real-time basis to make their forecasts. This need has led to the use of remote sensing methods. The gamma-ray survey methods described here are more efficient and reliable than ground-based measurements and can sample remotely. Because of the large spatial variations in snow, it is important to sample a large area, which can easily be done with remote sensing techniques but not with ground-based approaches.

In principle, microwave systems have the potential of providing a suitable remote sensing method. However, both microwave theory and the technology for this purpose are still being developed. Therefore, it is fortunate that another remote sensing technique, at the other end of the electromagnetic spectrum, is operational. Known as the airborne terrestrial gamma radiation technique, it is based on the snow cover's attenuation of terrestrially produced gamma-ray flux. This method is now providing highly reliable data in many countries. By its use, large local variations of the snow cover can be averaged along a flight course, and the available water mass can be predicted quickly.

The purposes of this review are

- To describe the physical principles and methods used,
- To explain some of the pertinent nomenclature,
- To present annotated references and
- To point out the potential and the limitations of the airborne gamma technique for determining SWE.

Advances in airborne gamma-ray snow surveying have been facilitated by intense developments for surveys of terrestrial-exposure maps and for uranium-rich ore deposits. The gamma technique has been applied under varied conditions, from the plains in the midwestern U.S. with only a few centimeters of snow, to the rugged mountains of Norway with several decimeters of snow. The U.S. National Weather Service has used this technique for monitoring watersheds in the midwest since 1978, and its success there has led to a planned expansion of the program to other water basins,

including those in the northeastern U.S. Worldwide interest was evident in 1979 at an international workshop in Norway on nuclear techniques in hydrology. Five countries (U.S.S.R., U.S., Canada, Norway and Finland) then reported using the airborne gamma method.

SNOW-WATER EQUIVALENT

The gamma-ray method detects the mass of water over the depth of the snow cover, which is usually reported as the snow-water equivalent in units of mass per unit area. The depth d and density ρ_s of a uniform snow cover are related by the simple equation

$$d = \text{SWE}/\rho_s. \quad (1)$$

The attenuation of gamma radiation is determined by the total mass, or SWE (or $d \times \rho_s$) and not by either d or ρ_s alone. This is shown in Figure 1, which is from one of the earliest measurements of natural gamma-ray transmissions through snow covers of different depths and densities (Sievert and Hultqvist 1952). Note that the same transmission rate of 40% occurs at a depth of 20 cm for a 0.40-g/cm³-density snow cover as at a depth of 80 cm for a 0.1-g/cm³-density snow cover, both cases having an SWE of 8 g/cm². Clearly, any one of the three curves shown is sufficient to give the information contained in all three.

Spatial variations of the snow cover are usually considered on three scales:

- On a macroscale or regional scale, with variations caused by dynamical meteorological conditions and geographical features and with characteristic distances of 10^4 – 10^5 m;
- On a mesoscale or local scale, with variations caused by wind, avalanches and snow depositional patterns and with characteristic distances of 10^2 – 10^3 m;
- On a microscale, with characteristic distances of 10 – 10^2 m.

There are over 3000 marked snow courses in the U.S. and Canada that are sampled several times each winter to yield SWE for water runoff estimates. The SWE of a region usually is obtained by averaging over relatively few representative ground locations for each snow course. This may lead to large errors (sometimes reaching 30%) because of the spatial variations over the measured courses and

because of extrapolations to areas not sampled at all. In contrast, in the airborne method the average SWE is obtained by sampling continuously over the entire flight line. In a typical case of a 20-km flight line, the sampled area might be 6 km². Since present systems are capable of storing the SWE values every 0.1 km, they can also measure the mesoscale variations of SWE. An example of such SWE variation over a 10-km open field course in the U.S.S.R. is shown in Figure 2.

Kogan et al. (1971) proposed the airborne method based on two interesting observations: 1) the existence in the earth's crust of a fairly constant source of high-energy gamma rays and 2) the deep penetrating power of high-energy gamma rays. Those with energies over 1 MeV have mean free paths in the atmosphere of 140 m. Therefore, these terrestrial gamma rays can be easily detected by scintillation crystals mounted on aircraft flying at low alti-

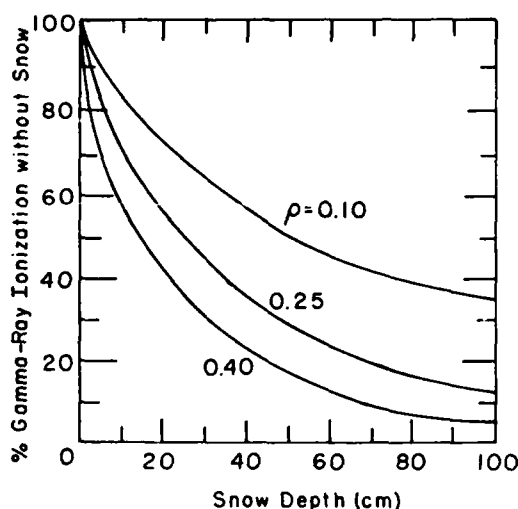


Figure 1. Gamma attenuation with depth of snow cover at three snow densities. (After Sievert and Hultqvist 1952.)

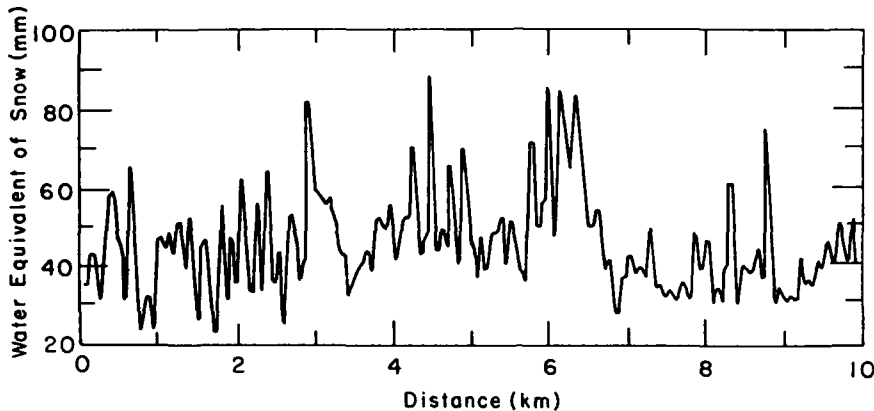


Figure 2. Variation of snow-water equivalent across an open field. (After Kogan et al. 1971.)

tudes. The attenuation of these rays, measured as the difference between the pre-snow values and the values with snow, produce a value for the SWE.

INTERACTION OF GAMMA RAYS WITH WATER SUBSTANCE

Gamma rays are high-frequency photons that originate from the decay of certain nuclei. Most of these photons have energies between 40 keV and 4 MeV, although gamma photons as low as 8 keV and higher than 4 MeV are known to exist. As a part of the electromagnetic spectrum, they form the transition region between the lower-frequency x-rays, produced by electron de-excitations, and the higher-frequency cosmic rays that come from outer space.

Of the more than a dozen different ways photons can interact with matter, only three are important for gamma rays: 1) the photoelectric process, dominant for low-energy photons, 2) the electron-positron pair production, which theoretically can occur only for energies greater than 1.02 MeV but which for water and other light elements is negligible until much higher energies, and 3) Compton scattering, in which the photon loses only part of its energy and survives as a lower-energy photon traveling in a different direction. The last process, which dominates for the gamma rays measured in airborne snow surveys, has to be understood to decode the observed gamma-ray spectrum.

The attenuation of a collimated gamma-ray beam is described by Lambert's law of absorption:

$$N = N_0 e^{-\mu' x} \quad (2)$$

where N_0 is the gamma flux (number per unit area per unit time) at a reference point and μ' is the linear absorption coefficient of the material. Since μ' depends on the density of the material ρ , we replace μ' by $\mu\rho$ and x by y/ρ . Equation 2 then becomes

$$N = N_0 e^{-\mu y} \quad (2a)$$

where μ is the mass-absorption coefficient and is a material constant that depends only on the gamma-ray energy. The effective path length y equals SWE for snow. The actual path in the equivalent water column D equals SWE/ρ_w .

Figure 3 shows the energy dependence of the total absorption coefficient for water from 10 keV to 10 MeV (Adams and Gasparini 1970). Note that the Compton contribution dominates above 0.1 MeV

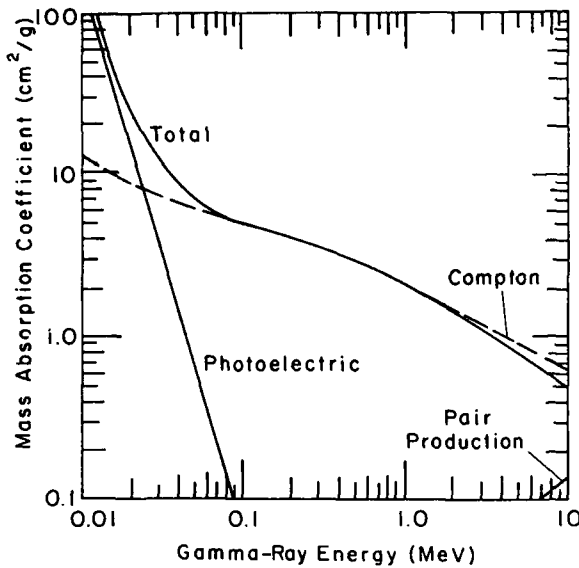


Figure 3. Mass absorption coefficient of water as a function of gamma-ray energy. From 0.1 to 3.0 MeV the total μ effectively coincides with the Compton μ . (After Adams and Gasparini 1970.)

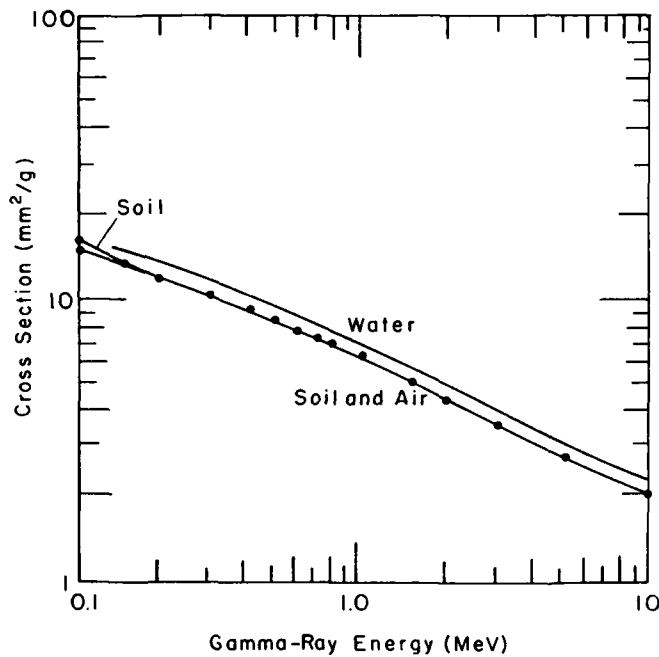


Figure 4. Gamma cross sections (mass absorption coefficients) for water, soil and air. (After Fritzsche 1982.)

and that pair production is negligible below 3.5 MeV. Compton scattering μ at a given energy depends on the electron density of the scattering medium n_e . But n_e is directly proportional to the *average Z/A* ratio of the constituent molecules (Z is the atomic number and A is the mass number). For compounds and mixtures of light elements, this average is 0.5. However, for ordinary water this average is 0.555 because the total atomic number is 10 and the total mass number is 18. For materials like dry soil, air and rock, which are mostly composed of light elements, it is 0.5. In the Compton-dominated energy range above 0.2 MeV, the mass absorption coefficient for air μ_a and the mass absorption coefficient for soil μ_g are therefore the same. On the other hand, the value for water μ_w is given by μ_w/μ_a , which equals 0.555/0.5, or 1.11. The energy dependence of the mass absorption coefficients is shown in Figure 4. As an example of the usefulness of these relations, we compute the water equivalent of the mass of air between the detector and the ground at an altitude of 150 m. At

standard temperature and pressure, the air-mass equivalent is 17.5 g/cm^2 . The equivalent SWE in the Compton energy region, therefore, is $17.5/1.11 = 15.3 \text{ g/cm}^2$.

SOURCES OF TERRESTRIAL GAMMA RADIATION

Gamma rays are emitted from the earth's surface due to the ubiquitous presence of 1) secondary, unstable isotopes produced by the naturally occurring radioactive series of elements, such as uranium and thorium, and 2) primeval radioisotopes with half-lives long enough to have survived since the solidification of the earth, such as uranium 235 and potassium 40. Table 1 lists the components of a typical terrestrial-radiation field and their fluxes as measured 1 m above ground. The total terrestrial flux is $10.4 \text{ gamma/cm}^2\text{-s}$, which is several times as large as the cosmic-ray flux at that level. These fluxes vary in opposite ways with altitude, as shown in Figure 5, which gives the results from Steamboat Springs, Colorado. Note that at ground level the terrestrial flux is six times the flux due to cosmic rays. Another noteworthy feature in the diagram is the total flux minimum at 4000 ft. It was the unexpected increase in flux with altitudes higher than that that gave the first indication of the existence of cosmic rays.

The average terrestrial-radiation intensity varies with geologic formations. It has been tabulated by country and varies from a low of $4.2 \mu\text{roentgen}/\text{hr}$ in India to a high of 9.5 in East Germany. The average for the entire U.S. is 5.4. In U.S. coastal plains it is half of that, and on the Colorado Plateau it is about twice the average value. The radiation observed above ground derives effectively from only the top 30 cm of soil or rock because the gamma rays emanating from deeper levels are dissipated.

Variation of gamma activity with time

The gamma activity at a particular locality varies with time due to three interrelated causes:

- Soil moisture, especially in the top 15–20 cm, is highly variable and will absorb some of the gamma rays before they leave the ground.
- The gases radon 222 and radon 220 (also called thoron) are the ancestors of the Bi^{214} and Ti^{208} isotopes, respectively. These gases can diffuse out of unfrozen soil because, if moisture is abundant, they may be concentrated in the water at higher concentrations than their radioactive equilibrium values. The radon concentration in the atmosphere is notoriously unpredictable because it varies with air circulation and other weather conditions.

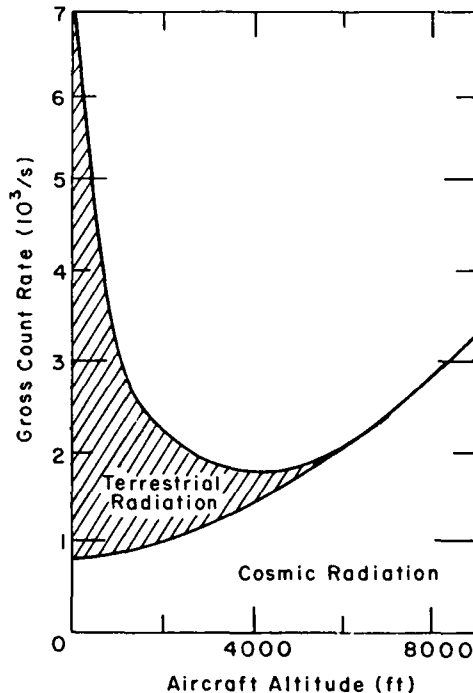


Figure 5. Relative cosmic and terrestrial components of measured gamma flux as a function of altitude at Steamboat Springs, Colorado. (After Bissell 1975.)

Table 1. Typical terrestrial gamma radiation field (Beck 1972).

Radiation source	Gamma flux at 1 m (count/ $\text{cm}^2\text{-s}$)
K^{40}	2.7
U^{238} + daughters	2.2
Th^{232} + daughters	4.1
Cs^{137} (1972)	0.8
Zr^{95} –Nb	0.4
Rn^{222} daughters in air	0.2

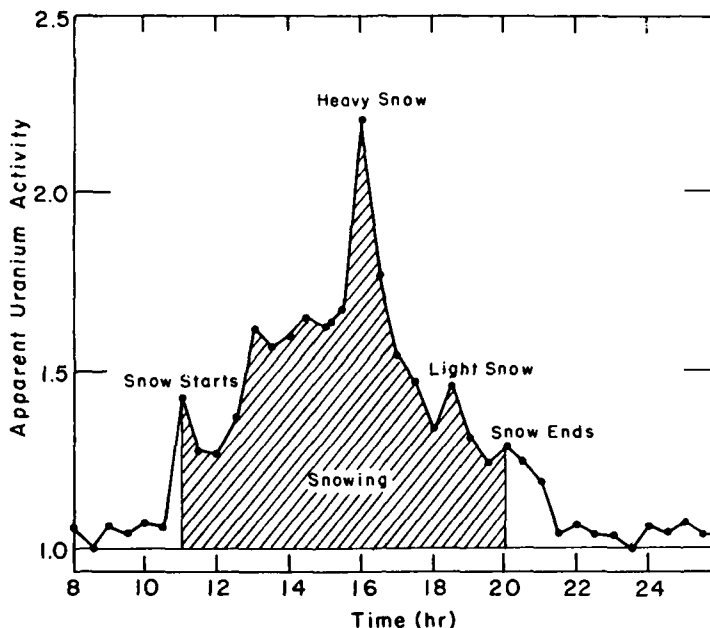


Figure 6. Apparent uranium activity on the ground during a snow-storm. (After Bissell 1975.)

- Radioactivity at ground level increases during and for a few hours following precipitation, as shown in Figure 6. This arises from Bi^{214} ions that are carried to the ground attached to the dust particles in precipitation.

Except for these complications, one can rely rather confidently on the constancy of terrestrial radiation. It provides the reference spectrum for the radiation observed when the ground is covered by a layer of snow.

The airborne spectrum

A typical airborne spectrum of the terrestrial radiation is shown in Figure 7. The three photopeaks or windows with the highest energy are the ones currently utilized in snow surveys. They are produced by the isotopes of Tl^{208} , Bi^{214} and K^{40} .

The highest energy peak at 2.62 MeV is due to Tl^{208} produced by the thorium 232 series, which is found with an abundance of 13 ppm in the earth's crust. This gamma-ray source accounts for over 50% of the energy released in this series, and because of its high energy, it is the one least attenuated. Also, it is not "diluted" with Compton gammas from the other peaks at lower energies.

The rather flat peak at 1.76 MeV results from the strongest of the many gamma rays produced by Bi^{214} . Bi^{214} is a short-lived (20-minute half-life) daughter product of Rn^{222} (3.8-day half-life), and both are part of the uranium 238 series, which occurs in the crust with an average concentration of about 2.5 ppm. However, the gammas registered in this peak are not constant for a given site because of the mobility of radon gas. Therefore, the intensity of this peak is not a reliable indicator of SWE unless an independent measurement of the extraneous radon contribution to the peak is made.

The gamma-ray source at 1.46 MeV is produced by K^{40} when this isotope, with a half-life of 1.39×10^9 yr, decays by electron capture and positron emission to an excited state of A^{40} , which happens in 11% of its decays. The crustal concentration of K^{40} is 2 ppm (i.e. 0.012% of K, which has an abundance of 2.5%). It is interesting to note that, although K was known to be a beta emitter in 1906, it was not until 1927 that its gamma emission was first detected (Kohlhorster 1928).

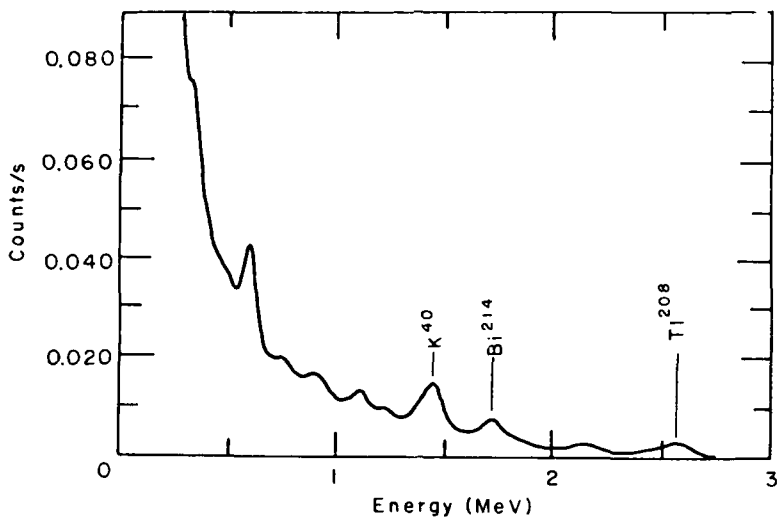


Figure 7. Airborne spectrum of energy peaks produced by radioactive elements in the ground. (After Dickson et al. 1981.)

Attenuation measurements near the ground

Ground measurements of SWE have been made by the gamma technique using artificial radioisotope sources as well as terrestrial radiation. Several years before the use of natural gamma rays were suggested, an experiment was conducted by the U.S. Army with an artificial gamma-ray source (U.S. Army Corps of Engineers 1955). Commonly used sources for artificial gamma rays are C^{60} , Cs^{137} and even Kr^{85} isotopes. Snow density profiles as well as SWE have been measured this way. The results from one of the early ground experiments using total terrestrial radiation is shown in Figure 8. Note the precision with which SWE could be determined over different ranges of D (Bissell and Peck 1973). These measurements were made with a small portable detector mounted on a boom 2 m above the ground, insulated with 5 cm of Styrofoam, and maintained at a nearly constant temperature throughout the snow season. The effective "look area" of the detector was several square meters, and its output pulses were accumulated by a scalar for periods of one hour.

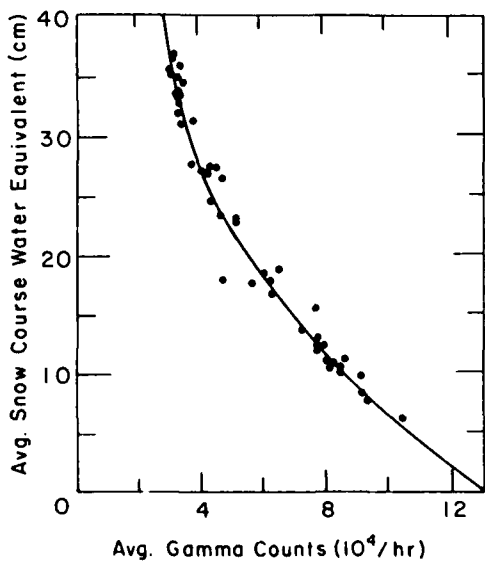


Figure 8. Snow-water equivalent vs one-hour gross gamma counts, measured 2 m above the ground. (After Bissell and Peck 1973.)

TECHNICAL ASPECTS OF AIRBORNE GAMMA-RAY SURVEYS

Airborne gamma-ray surveys differ from the ground-based observations in several important ways. Due to the different geometric relationships between sources and detectors, illustrated in Figure 9, the counting rate is proportional to an exponential integral rather than to a pure exponential.

The gamma rays can be collected by a sophisticated spectrometer, which has the capability not only of measuring gamma intensities, but also of determining changes in the shape of the gamma-ray spectra.

By comparing the absorption of gamma rays at two or more energies and knowing the air layer thickness, it is possible to deduce the SWE without a pre-winter measurement. The gamma rays are diminished by absorption in the air layer beneath the aircraft. This increases the error in the measurement due to both the uncertainty in the amount of air and the lower count rate.

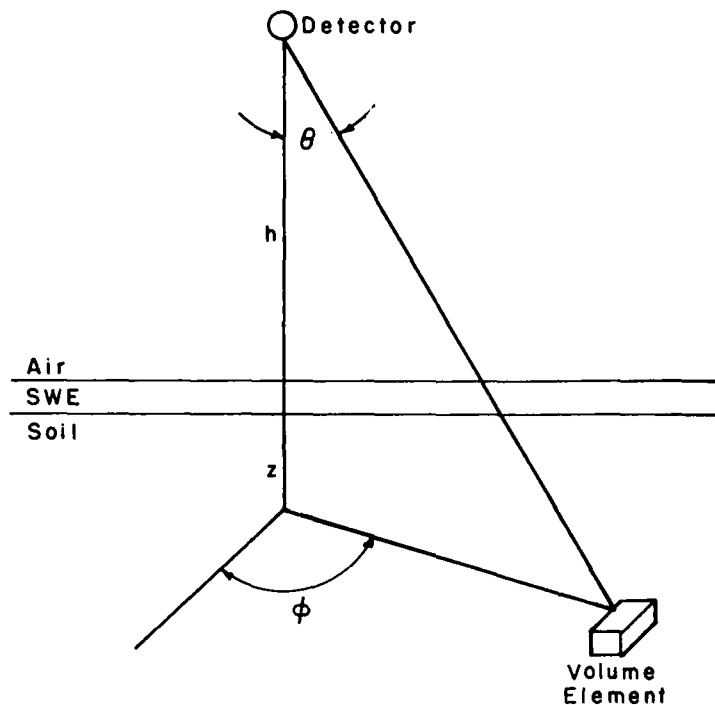


Figure 9. Geometric relationship for aerial gamma measurement (Fritzsche 1982.)

Equation for the transport of uncollided gamma rays

The flux of uncollided gamma rays N arriving at a detector at an effective altitude H above the ground is given by

$$\begin{aligned}
 N &= \frac{CR}{A_0} = S \int_0^\infty dz \int_0^{\pi/2} d\theta \int_0^{2\pi} \frac{R(\theta) e^{-(\mu_a H + \mu_w SWE) \sec \theta} e^{-\mu_g Z \sec \theta} \tan \theta}{4\pi} d\phi \\
 &= \frac{S}{2\mu_g} \int_0^{\pi/2} R(\theta) e^{-(\mu_a H + \mu_w SWE) \sec \theta} \sin \theta d\theta
 \end{aligned} \tag{3}$$

where CR = unscattered gamma count rate

$R(\theta)$ = angular detector response

A_o = effective detector area

S = soil activity

θ and ϕ = angles identified in Figure 9

μ_g = soil-mass absorption coefficient

μ_a = air-mass absorption coefficient

μ_w = snow-mass absorption coefficient

Z = effective vertical distance below the surface of the volume element of soil (Fig. 9), or the actual distance z times the density of the soil

H = effective detector height .

H equals the physical altitude h times the density of air, which is obtained from pressure and temperature measurements.

If the detector response is independent of θ , then $R(\theta)$ equals 1, and we can rewrite eq 3 simply as

$$N = \frac{S}{2\mu_g} E_2(q) \quad (4)$$

where q is $\mu_a H + \mu_w \text{SWE}$ and E_2 is the second value of the exponential integral of the n th kind defined as the integral

$$E_n(q) = \int_1^{\infty} \frac{e^{-qx}}{x^n} dx \quad (5)$$

If $R(\theta)$ equals $\cos \theta$, then $E_3(q)$ results instead of $E_2(q)$. The flux N is proportional to the soil activity and inversely proportional to the attenuation coefficient of the soil.

Equation 4 is based on two idealized assumptions. The first is that the soil radiation is uniformly distributed in an infinite halfspace below the earth's surface, although only the top 0.30 m really matter. The second is that the radiation enters the detector from an infinitely extending plane, equivalent to a cone angle of 90°. For other source-detector geometries, theoretical values for N are less. (For example, when the area "seen" by the detector is confined to a 65° rather than a 90° cone angle, N is only 90% of the value given by eq 4.)

Reduction coefficients and the "working" equation

In actual field applications the q dependence is given by a function that lies between E_2 and E_3 . It is customary, therefore, to approximate the $E(q)$ function by a pure exponential expression. Instead of using the true mass attenuation coefficients (Table 2), one determines for a particular snow course the coefficients for an exponential best fit of the experimental variation of N with the effective air height H . These are called reduction coefficients and are designated by α_a to indicate that they are to be multiplied by the effective air height H .

The presence of soil moisture increases the attenuation in two ways. First, the radioactivity of the soil per unit volume is reduced, and second, the moisture itself attenuates the radioactivity 11% more effectively than the soil materials. Including the effect of the moisture content of the soil and μ and S , the "working" equation is

$$N = \frac{S_o}{2 \mu_{go} (1 + 1.11 M)} e^{-\alpha_a (H + 1.11 \text{SWE})} \quad (6)$$

Table 2. Mass attenuation coefficients and half thicknesses $X_{1/2}$ for air, water and rock at the photopeak energies of K^{40} , Bi^{214} and Tl^{208} .

Photon energy (MeV)	Mass attenuation coeff.			Half thickness $X_{1/2}$		
	Air	μ (cm ² /g)	Rock	Air (m)	Water (cm)	Rock (cm)
1.46 (K^{40})	0.0526	0.0585	0.0528	102	11.8	5.25
1.76 (Bi^{214})	0.0479	0.0532	0.482	112	13.0	5.75
2.62 (Tl^{208})	0.0391	0.0433	0.0396	137	16.0	7.00

where $X_{1/2} = 0.693/\mu$ and the density (g/cm³) of materials under standard conditions are 0.001293 for air, 1.0 for water and 2.5 for rock. Air is 75.5% N, 23.2% O and 1.3% Ar by weight.

where M = soil moisture expressed as percentage of dry soil

S_o and μ_{go} = radioactivity and mass absorption coefficients of dry soil, respectively

α_a = reduction coefficient to be determined by calibration procedures.

The exponent can also be expressed as $-\alpha_w$ (0.9 H + SWE).

The measured values for α_w shown in Table 3 were obtained from the slope of the log of the uncollided or stripped gamma-count rates versus q . Stripped count rates are derived from actual counts by removing the counts that arise from the Compton-scattered photons of different energies. The procedure for doing this uses stripping ratios—the ratios of counts detected in window A to counts detected in window B from a pure gamma source corresponding to the energy of window A. These stripping ratios, which are linearly increasing functions of SWE, are determined for each detection system by experiments carried out over calibration pads containing known concentrations of each of the three gamma sources. Figure 10 shows the fit to E_2 and exponential curves of experimental values of N , with the background corrected and stripped, for the K peak for the altitude range of 50–250 m.

Techniques for determining SWE

A number of techniques have been proposed for obtaining SWE from radiational spectra. Some of these are listed in Table 4 together with the appropriate equations for relating N to SWE. All the methods use ratios of counts because, for a snow survey as opposed to a uranium survey, one is not interested in S per se. Since μ varies with gamma energy, these equations apply, strictly speaking, only to one particular gamma-ray count at a time. However, by the choice of

Table 3. Values for α_w (cm⁻¹ × 10⁻⁴).

	Steamboat Springs, Southern Ontario (Glynn & Grasty 1980)	Colorado (Bissell 1975)	Luverne, Minnesota (Bissell 1975)
K	722	703	704
Tl	591	529	571

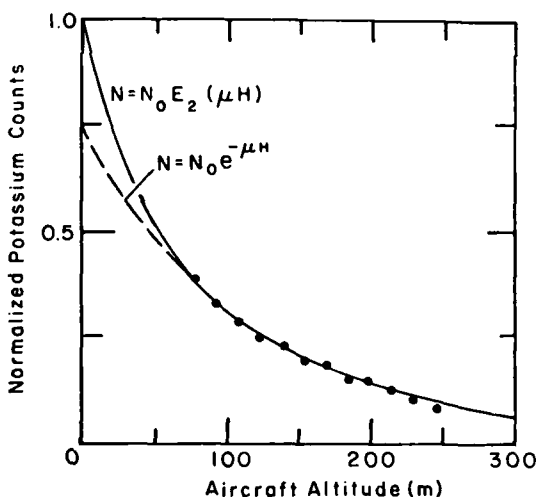


Figure 10. Potassium peak variation with aircraft altitude: measured points and fits to an exponential integral and to a pure exponential. (After Grasty 1979.)

Table 4. Techniques of SWE measurements.

Name	Equation	Parameters to measure
(1) Snow and presnow (standard two flights)	$\frac{N_s}{N_p} = \frac{E_2(\mu_a H_s + \mu_w SWE)}{E_2(\mu_a H_p)} \times \frac{1 + 1.11 M_p}{1 + 1.11 M_s}$	H_p, H_s M_p, M_s
(2) Two altitudes (same snow)	$\frac{N_{s,1}}{N_{s,2}} = \frac{E_2(\mu_a H_1 + \mu_w SWE)}{E_2(\mu_a H_2 + \mu_w SWE)} \frac{E_2(\mu_a H_2)}{E_2(\mu_a H_1)}$	H_1, H_2
(3) Two different angle intervals (one flight)	$\frac{N_{s,1}}{N_{s,2}} = \frac{E_2(\mu_a H + \mu_w SWE)}{\cos \theta E_2 \left[\frac{\mu_a H_2 + \mu_w SWE}{\cos \theta} \right]} - 1$	H
(4) Two photopeaks (one flight)	$\frac{N_{s,1}}{N_{s,2}} = \frac{S_{0,1} \mu_{g,2} E_2 (\mu_{a,1} H + \mu_{w,1} SWE)}{S_{0,2} \mu_{g,1} E_2 (\mu_{a,2} H + \mu_{w,2} SWE)} \frac{E_2 \mu_{a,2} H}{E_2 \mu_{a,1} H}$	$H, \frac{S_1}{S_2}$

suitable average μ values, the first three equations have also been used for gross counting techniques. Techniques 1 and 2 are also known as incremental methods and 3 and 4 as direct methods. The formula for technique 3 corresponds to two detector angles; detector 1 counts rays that make an angle of less than θ with the vertical direction and detector 2 counts rays outside of this angle.

In evaluating the comparative advantages of each method, the following points should be considered:

- The number of parameters that must be measured (last column of Table 4).
- The magnitude of the "counting error." The accuracy decreases for a smaller detected intensity. Thus technique 2 would be useful only if enough signal is left at the higher altitude. In practice this would restrict the method to D values of 10 cm or less. In technique 3 the "counting" errors increase even in the gross counting mode because only part of the available rays are being selected for measurement.
- The difficulty of accurate soil-moisture determinations required for technique 1.
- The cosmic-ray activity variation with altitude required for technique 2.

Further research is needed for the development of the direct techniques 3 and 4. These have significant advantages over the two-flight method because they do not require pre-snow flights or separate soil-moisture measurements, and of course, the errors in duplicating flight lines are eliminated.

Two-flight surveys

In the most common two-flight technique, the background spectrum for a snow-free flight line is recorded in the fall (at an altitude H_p and with soil moisture content M_p). The spectrum over the same flight line is obtained again (at an altitude H_s and soil moisture content M_s) after the snow has been deposited in the winter (technique 1, Table 4.) For a given detector system, $N_s/N_p = CR_s/CR_p$ and then, if H_s equals H_p , the appropriate equation becomes

$$SWE = \frac{1}{\alpha_w} \left[\ln \frac{CR_p}{CR_s} - \ln \left(\frac{1 + 1.11 M_s}{1 + 1.11 M_p} \right) \right] \quad (7)$$

where α_w is the water reduction coefficient appropriate to the equipment and location.

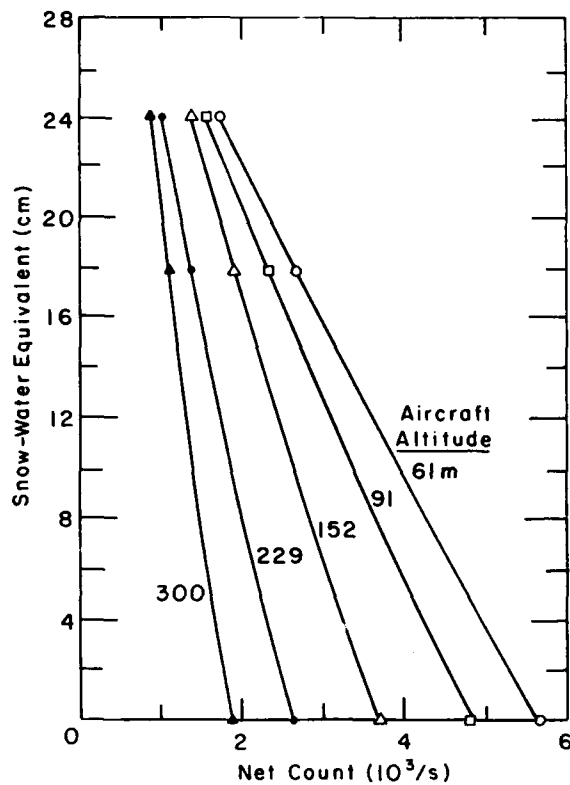


Figure 11. Snow-water equivalent vs net count rate at altitudes from 61 to 300 m. (After Peck et al. 1980.)

Flight altitude

The measurements typically take place from aircraft flying 50–300 m above the ground along routes 10–20 km in length. The altitudes flown are lowest in the U.S.S.R., about 50–100 m. In Canada the standard altitude is 120 m, and in the U.S. it is generally 150 m. The effect of altitude on the curve of D vs N is shown in Figure 11. These observations were taken at the 7-km research test site at Steamboat Springs, Colorado.

The choice of a flying altitude is the result of a compromise. Lower altitudes produce a smaller uncertainty in D for a given uncertainty in N , δN , because the bigger N reduces the inherent statistical error and because the smaller slope of the D vs N curve reduces the uncertainty in D associated with a given δN . However, it is more difficult and dangerous to fly at low altitudes, and regulations in the U.S. require higher flight altitudes than in some of the other countries.

Instrument package and determination of D

Figure 12 shows an example of an operational snow spectrum obtained by Carroll and Vadnais (1980) for a 5-cm snow cover. They used a third-generation detection package that consisted of five downward-looking NAI (Tl) scintillation crystals and two upward-looking crystals. The purpose of the latter was to measure the Bi^{214} gamma rays coming from atmospheric radon. The detectors plus the computer weigh about 550 pounds.

The 20-km flight course was 300 m wide and thus covered approximately 6 km² of snow cover. The average D measured on the ground for this flight line was 5.1 ± 1.5 cm. Three independent D values were determined for each of two flights. The K peak gave 5.1 and 5.3 cm, the Tl peak gave 5.6 and 5.8 cm, and the gross count (between 0.42 and 3.0 MeV) gave 3.0 and 3.3 cm. The underestimate of the gross count can be ascribed to the Rn build up in the ground. Grasty* found in a more recent experiment that the count in the uranium window for fine clay soil decreased with the drying of the soil.

* Personal communication.

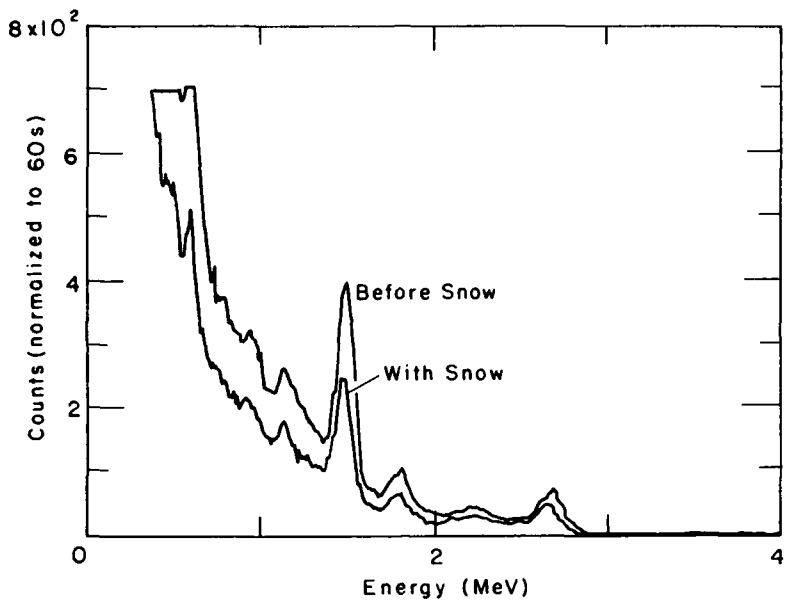


Figure 12. Terrestrial gamma radiation spectra—one-minute counts vs gamma energy—for no snow (background) and for an average D of 5 cm of snow. (After Carroll and Vadnais 1980.)

By comparing this observation with sandy soil over the same range, he concluded that the radon was leaking out faster than its natural equilibrium replenishment rate in the clay soil. This causes the snow measurement to have a larger radon component than would be expected from pre-snow measurements and would thus lead to an underestimate of SWE. The gross count recorded at frequent intervals along the flight path was particularly valuable for determining the variability of the snow cover. In general it is this mode that gives the best value for the mean areal snow cover when D is greater than 15 cm.

The K^{40} gamma peak at 1.461 MeV is the most pronounced one in the spectrum and therefore gives the most accurate value of D for shallow snow covers up to a D value of 10 cm. For thicker snow covers, the Thallium²⁰⁸ peak at 2.615 MeV is more reliable.

The Bi^{214} photopeak at 1.765 MeV is used only for monitoring the radon contribution to the background counts. The counts in the cosmic window above 3 MeV are used to help separate the cosmic background flux. The 512 channel spectra were recorded on magnetic tape at the end of each flight. The background counts were recorded at 20-s intervals, equivalent to 1 km. The over-snow spectrum was recorded at 5-s intervals, equivalent to 0.25-km stretches of snow. The detection system is actually capable of recording every 2 s, which is equivalent to a 100-m-long strip of snow.

Background counts

The background counts are determined most readily by flying over a nearby lake, since the water will attenuate all the gamma rays emitted by the underlying ground. If no such body of water is available, flights of multiple altitudes are necessary. Calibrating the spectrometer requires the experimental determination of more than 20 parameters, including stripping coefficients and basic system sensitivity. This is usually carried out over artificially constructed simulation pads containing known concentrations of K, Th and U.

Spectral shape methods: single flights

To use the enormous amount of information available in multichannel spectra, it was suggested that D should be obtained from an analysis of the spectrum shape. For example, a modified version of technique 4 has been tested by Grasty (1982a). He compared the counts in the low-energy window

(0.72–1.36 MeV) with the counts in the potassium window (1.36–1.56 MeV). For a pure potassium source, this count ratio varies linearly with D , from 1.30 for no snow to 1.90 for $D = 14$ cm. This method takes advantage of the Compton transformation of potassium gamma rays into lower-energy gamma rays. The low-energy window minimum is chosen at 0.72, to be above the Cs¹³⁷ gamma ray peak at 0.66 MeV. Cs¹³⁷, a residue of atomic weapons testing, is present in almost all airborne measurements of radioactivity.

Another promising development is the spectral component method suggested by Dickson et al. (1981). They have shown that the spectra of each of the three radioelements (U, Th and K) are made up essentially of only two significant spectral components. The proportions of these components vary directly with the amount of absorbing material between source and detector. Thus, a spectral shape analysis can yield D if H is known. However, this method has only been tested up to about D equal to 10 cm.

ACCURACY OF D

For the airborne gamma-ray technique to qualify for operational use for forecasting of snowmelt runoff, it must be able to deliver values of D to within an rms error of 1 cm. The obtainable accuracy of D depends on the terrain. For agricultural areas it has been possible to reduce the rms error to 0.8 cm. Over forested environments, however, the rms error is about twice as large due to the presence of biomass and boggy ground. This result is, nevertheless, better than not knowing whether D is 4 or 40 mm. The accuracy is expected to improve with years of experience for a given snow course.

Bissell (1975) conducted a comprehensive study of the measurement accuracy of the technique under conditions anticipated in the U.S. He drew these conclusions:

- The working equation could be trusted for accuracy only over the range of D values used in the calibration.
- The statistical error in the counts is significant and increases with D and H .
- Errors due to soil moisture variation on different days can be of serious concern.
- The spatial variability of the snow cover can produce significant D errors due to the nonlinearity of the N vs D curve. However, in practice these errors will be much reduced because of their inclusion in the N – D calibration curves.

Possible sources of error

for any snow course

Counting errors due to statistical fluctuations can be reduced by slower flights, longer flight lines, lower altitudes, and larger detection packages. One would expect that, in consideration of this kind of error, which is always associated with random event processes, the gross (sometimes called the integral or total) count method would be the most precise.

Errors in the measurement of calibration constants are the result of the more than 20 such constants (including the stripping coefficients) that have to be determined. These "constants" are themselves functions of the magnitude of the attenuation.

Errors arise from the determination of the background radiation from the aircraft, the instruments themselves and from cosmic rays.

Spurious radiation from daughter products of radon and thoron varies with the conditions of the ground and the convection of the atmosphere. Because it is the most predictable of all errors, many methods have been proposed to determine the Rn contribution to the spectrum, including over-lake flights, dual-altitude flights, dual detectors (up- and down-looking detectors), spectrum shape analyses, and air filters to catch radioactive-radon daughter products. According to Peck et al. (1980), over-lake flights and spectrum shape analysis are the most promising ones, but dual detectors are used in the current operational systems. The 0.352-MeV gamma ray from Pb²¹⁴ is totally absorbed in 150 m of air, and therefore a separate monitoring of this gamma ray can help keep track of spurious Rn.

Table 5. Relative standard errors of snow surveying with various degrees of snow cover nonuniformity and various average snow-water equivalents along the flight line. (After Nikiforov et al. 1980.)

Coefficient of variation	Average snow-water equivalent (mm):	Relative standard error (%)								
		200	500	700	1000	1500	2000	3000	4000	6000
0		3.3	2.6	7.0	34	>100	>100	>100	>100	>100
0.25		3.6	2.8	4.9	20	>100	>100	>100	>100	>100
0.50		4.3	3.1	3.9	6.5	16.0	45	>100	>100	>100

D is variable along snow courses, especially for distances smaller than those corresponding to the minimum time for count accumulation. Because attenuation is an exponential function, the average for a variable snow cover will not be an arithmetic mean. The areas with shallow snow coverings will dominate, leading to an underestimation of SWE. Errors associated with non-uniform snow covers depend both on the amount of variation, expressed by a variation coefficient, and on the average depth of the snow cover (Table 5).

The nonplanar topography of a snow course leads to errors.

Errors are associated with using a fitted exponential function rather than the appropriate exponential integral function. The ground truth values used in such fittings are themselves subject to errors because of the inherent spatial variability of SWE, extrapolation of density values, snow tube errors, depth measurement errors, biases of ground crews in estimating percentage of area covered by snow, and areas of ground ice.

Errors in the measurement of the air mass between ground and detector are called analog errors.

Additional sources of errors for the two-flight method

Navigation errors arise in reflying snow courses including altitude errors (also called tracking errors). Variations of the ground moisture and the radon content of the atmosphere between measurements on subsequent flights also cause errors. A 5% error in *M* leads to a 2% error in SWE.

Additional time-dependent errors

Errors are incurred if measurements are made too soon after precipitation has occurred, because the short-lived, radioactive particles just deposited have not yet decayed. These errors have all been thoroughly examined during the research and field study phases, and certain qualitative conclusions are generally known.

Despite all these possible sources of error, airborne forecasts of runoff have been reported that were closer to the actual runoff than the ground-based forecasts. It is estimated that five years of accumulated experience is required in a given region for the technique to yield the best value for SWE for forecasting. Even more years of experience are necessary if a flight-line SWE value is to serve as a runoff index.

OPERATIONAL USE

The airborne gamma technique was first put into operation in the Soviet Union in 1971 (Vershinian and Dimakyan 1971) after years of extensive research on the method at the Soviet Hydrological Institute. The U.S. National Weather Service (NWS) initiated an operational program over the northern plains states in 1979 based on a research program that began in 1969 (Peck et al. 1980). One of the primary aims of this program was to provide near-real-time SWE data as an aid for snowmelt forecasting. Data are collected over a network of approximately 350 flight lines in North and South Dakota and Minnesota. These data are used by the NWS River Forecast Centers in Kansas City and

Minneapolis for regional spring flood outlooks. Ground-based soil-moisture measurements are included in the instrument calibration procedures. The data are disseminated to NWS offices in 30–45 minutes after the aircraft lands at noon and in the evening of each day of operation.

The Geological Survey of Canada (GSC) also developed its own airborne radiometric system with a 1-s interval recording capability. In a joint U.S.–Canadian experiment over the prairies of central Saskatchewan the week of 15 February 1982 (Carroll et al. 1983), the SWE results for the two systems were compared for snow covers of from 21 to 76 mm over 17 flight lines. The results were computed by weighting the values for the K, Tl and GC (gross count) windows with weighting factors of 0.35, 0.52 and 0.13, respectively. These weights were derived by minimizing the variance of the weighted SWE. The ground measurements had an rms error of 10 mm. This poor precision resulted from using the ground values collected over an area of less than 2 m² to infer a mean areal SWE over an area of 4–8 km². The airborne results of NWS and GSC agreed with each other to within an rms error of 4.5 mm, the Canadian results being about 1.5% lower than the American. They agree with each other more closely than either does with the ground observations. It was also found that the additional detectors, carried aloft by the Canadian planes for improving the counting statistics, did not improve the overall accuracy because the air-mass measurement error is larger than the counting statistics error.

The NWS system operated at first in six states (North and South Dakota, Montana, Iowa, Kansas and Minnesota) and then planned to expand the service to 10 additional states from Michigan to Maine.

CONCLUSIONS

Airborne surveys provide a rapid and far-ranging measurement capability for determining SWE. These surveys are relatively free of the problems of small-scale sampling caused by local drifting and redistribution of snow that plagues ground-based networks. They provide data that effectively supplement areal snow maps from satellites and ground observations.

Factors that may limit the usefulness of the technique include low radioactivity of the ground, very thick snow covers, rugged terrain, and insufficient technical and administrative support. The areas of application may increase with the development of more sensitive detectors and spectrum analyzers and further progress with the spectral shape-analysis method. The development of the equipment and technique has now progressed to the point that soil-moisture surveys themselves are being successfully conducted by the airborne gamma technique. More-accurate values for an entire snow-covered region could produce major improvements in hydrologic forecasting, snow-hazard evaluation, agricultural yield assessment and weather forecasting.

ANNOTATED BIBLIOGRAPHY

Adams, J.A.S. and P. Gasparini (1970) *Gamma-Ray Spectrometry of Rocks*. Amsterdam: Elsevier. (Comprehensive and authoritative compendium.)

Beck, H.L. (1972) The physics of environmental gamma radiation fields. *Proceedings of the Second International Symposium on the Natural Radiation Environment, Houston, Texas*.

Bissell, V.C. (1975) Accuracy evaluation of airborne snow water equivalent measurements using terrestrial gamma radiation spectral peaks. University of Maryland PhD thesis in Civil Engineering. (Thorough analysis and very readable.)

Bissell, V.C. and E.L. Peck (1973) Monitoring snow water equivalent by using natural soil radioactivity. *Water Resources Research*, 9: 885–890. (Report of field observations.)

Carroll, T.R. and K.G. Vadnais (1980) Operational airborne measurement of snow water equivalent using natural terrestrial gamma radiation. *Proceedings, Western Snow Conference, Laramie, Wyoming*, p. 97–106. (Example of operational use in U.S.)

Carroll, T.R., J.E. Glynn and B.E. Goodison (1983) A comparison of U.S. and Canadian airborne gamma radiation snow water equivalent measurements. *Proceedings, Western Snow Conference, Vancouver, Washington*, p. 27–37. (Progress on method.)

Dickson, B.H., R.C. Bailey and R.L. Grasty (1981) Utilizing multi-channel airborne gamma-ray spectra. *Canadian Journal of Earth Sciences*, **18**(12): 1793–1801. (Potential use for single-flight method.)

Edrestoel, G.O. (1980) Principle and method for measurement of snow water equivalent by detection of natural gamma radiation. *Hydrological Sciences Bulletin*, **25**: 77–83. (Good introduction for different methods.)

Fritzsche, A.E. (1982) The National Weather Service gamma snow system physics and calibration. NWS-8201 December 1982, EG&G Energy Measurement Group. (Physics of detection and calibration.)

Glynn, J.E. and R.L. Grasty (1980) A calibration procedure for airborne gamma ray snow surveys. *Proceedings, Western Snow Conference, Laramie, Wyoming*, p. 120–127. (Example of a calibration experiment.)

Goldstein, H. (1971) *Fundamental Aspects of Reactor Shielding*. Johnson Reprint. (Compton scattering treatment and buildup factor reference.)

Grasty, R.L. (1979) Gamma ray spectrometric methods in uranium exploration theory and operational procedures. *Geophysics and Geochemistry in the Search for Metallic Ores* (Peter J. Hood, Ed.). Also (1979) Geological Survey of Canada, Economic Geology Report 31, p. 147–161. (Gamma ray and physics background.)

Grasty, R.L. (1982a) Direct snow water equivalent measurement by air-borne gamma-ray spectrometry. *Journal of Hydrology*, **55**: 213–325. (Test of single flight technique for 142-mm D .)

Grasty, R.L. (1982b) Utilizing experimentally derived multi-channel gamma-ray spectra for the analysis of airborne data. *Symposium on Uranium Exploration Methods, Paris, 1–4 June 1982*.

Grasty, R.L. (1983) *Radiation Sources*. Geos, Department of Energy, Mines and Resources, 12, 1–5. (Popular reference.)

Goodison, B.E., H.L. Ferguson and G.A. McKay (1981) Measurement and data analysis. In *Handbook of Snow* (Gray, D.M. and Male, D.H., Eds.), New York: Pergamon Press, p. 235–243. (Remote sensing of snow cover.)

Kogan, R.M., I.M. Nazarov and D. Fridman (1971) *Gamma Spectrometry of Natural Environments and Formations*. Moskva 1969, Israel Program for Scientific Translations, Jerusalem. (Most comprehensive background reference.)

Kohlhorster, W. (1928) Gammastrahlen an Kaliumsalzen. *Naturwiss*, **16**(2): 28. (Discovery of the important potassium gamma radiation.)

Meier, M.F. (1980) Remote sensing of snow and ice. *Hydrological Sciences Bulletin*, **25**: 307–330. (Specific capabilities of various remote sensing methods.)

Nikiforov, M.V., N.N. Pegoev and A.N. Stroganov (1980) Aerial gamma survey of snow cover and soil moisture. *Hydrological Sciences Bulletin*, **25**: 85–91.

Peck, E.L., T.R. Carroll and S.C. Vandemark (1980) Operational aerial snow surveying in the United States. *Hydrological Sciences Bulletin*, **25**: 51–62.

Rango, A. (1979a) Review of remote sensing capabilities in snow hydrology. *American Society of Civil Engineers (ASCE) Convention and Exposition, Boston, 2–6 April 1979*.

Rango, A. (1979b) Remote sensing of snow and ice: A review of research in the U.S. 1975–1978. Goddard Space Flight Center, NASA Technical Memorandum 79713.

Siever, R.M. and B. Hultqvist (1952) Variations in natural γ -radiation in Sweden. *Acta Radiologica*, **37**: 388–398. (Earliest reference.)

NASA (1982) Plan of research for snowpack properties remote sensing, (PRS)2. Snowpack Properties Working Group, Goddard Space Flight Center. (Report of a committee of specialists.)

U.S. Army Corps of Engineers (1955) Development and test performance of radioisotope-radiotelemetering snow-gage equipment. Pacific Division, San Francisco, California, Civil Works Invest. Proj. CWI-170, 74, p. 8. (Early use of gamma technique with artificial sources.)

Vershinina, L.K. and A.M. Dimakyan (Ed.) (1971) Determination of the water equivalent of snow cover, methods and equipment. Leningrad 1969, Israel Program for Scientific Translations, Jerusalem. (Collection of papers.)

Zotimov, N.V. (1968) Investigation of a method of measuring snow storage by using the gamma radiation of the earth. *Soviet Hydrology: Selected Papers*, 3: 254-266. (Early ground measurements and distribution of radiation in earth layer.)

REPORT DOCUMENTATION PAGE

Form Approved
OMB No. 0704-0188

Public reporting burden for this collection of information is estimated to average 1 hour per response, including the time for reviewing instructions, searching existing data sources, gathering and maintaining the data needed, and completing and reviewing the collection of information. Send comments regarding this burden estimate or any other aspect of this collection of information, including suggestion for reducing this burden, to Washington Headquarters Services, Directorate for Information Operations and Reports, 1215 Jefferson Davis Highway, Suite 1204, Arlington, VA 22202-4302, and to the Office of Management and Budget, Paperwork Reduction Project (0704-0188), Washington, DC 20503.

1. AGENCY USE ONLY (Leave blank)	2. REPORT DATE April 1991	3. REPORT TYPE AND DATES COVERED	
4. TITLE AND SUBTITLE Remote Sensing of Snow Covers Using the Gamma-Ray Technique			5. FUNDING NUMBERS PE: 6.27.84A 6.27.30A PR: 4A762784AT42 4A762730AT42 TA: FS and D WU: 003 004
6. AUTHORS Elmer L. Offenbacher and Samuel C. Colbeck			8. PERFORMING ORGANIZATION REPORT NUMBER CRREL Report 91-9
7. PERFORMING ORGANIZATION NAME(S) AND ADDRESS(ES) U.S. Army Cold Regions Research and Engineering Laboratory 72 Lyme Road Hanover, New Hampshire 03755-1290			10. SPONSORING/MONITORING AGENCY REPORT NUMBER
9. SPONSORING/MONITORING AGENCY NAME(S) AND ADDRESS(ES) Office of the Chief of Engineers Washington, D.C. 20314-1000			12a. DISTRIBUTION/AVAILABILITY STATEMENT Approved for public release; distribution is unlimited. Available from NTIS, Springfield, Virginia 22161
11. SUPPLEMENTARY NOTES			
12a. DISTRIBUTION/AVAILABILITY STATEMENT Approved for public release; distribution is unlimited. Available from NTIS, Springfield, Virginia 22161		12b. DISTRIBUTION CODE	
13. ABSTRACT (Maximum 200 words) This report reviews various aspects of the use of natural gamma-ray emissions to determine the mass of snow covering the ground. The interactions of gamma rays with water mass are described, along with the various sources of gamma radiation from the ground. Different possible techniques for measuring gamma radiation are described. Each has advantages and disadvantages in obtaining the desired result. The sources of error and the use of this method are described.			
14. SUBJECT TERMS Aerial surveys Detectors Gamma ray		Snow Snow cover	Snow surveys Snow water equivalent
15. NUMBER OF PAGES 26		16. PRICE CODE	
17. SECURITY CLASSIFICATION OF REPORT UNCLASSIFIED	18. SECURITY CLASSIFICATION OF THIS PAGE UNCLASSIFIED	19. SECURITY CLASSIFICATION OF ABSTRACT UNCLASSIFIED	20. LIMITATION OF ABSTRACT UL